Measurement Notes

Note 61

November 2008

# Windscreen Shield Monitoring Using a Spiral Transmission Line

Everett G. Farr. W. Scott Bigelow, and Leland H. Bowen
Farr Research, Inc.

Carl E Baum
University of New Mexico

William D. Prather
Air Force Research Laboratory / DE

## Abstract

In this paper we investigate two new methods of testing the integrity of EMI gaskets surrounding aircraft windscreens. This is normally accomplished by placing an RF source on the exterior of the window, and checking for fields leaked into the interior. Currently used methods require disassembly of portions of the interior of the cockpit, so we look for more convenient methods using a Spiral Transmission Line (STL) on the interior. The first method uses a second STL on the exterior, which allows us to successfully locate the position of a leak using time domain measurements. The second method uses a stripline on the exterior, similar to the "blanket" that is currently used. In this configuration, we observed a 30-40 dB difference between the leaky and sealed configurations, over a frequency range of 50-200 MHz.

## CONTENTS

## I. Introduction

Many aircraft are hardened against the effects of various forms of high power electromagnetic waves, including Electromagnetic Pulse (EMP), High Power Microwaves (HPM), High Intensity Radio Frequency (HIRF), and lightning. These aircraft typically have electrically conducting coatings on their windows, with conducting gaskets that form an electromagnetic seal with the fuselage. These gaskets wear out over time, and must be periodically replaced. We consider here methods for testing the integrity of these gaskets.

Gasket integrity is normally tested by placing an RF source on the exterior of the window, and checking for leaked fields on the interior. In principle, this is a straightforward process; however, newer aircraft present some challenges. In some cases, one must remove a significant amount of molding to get access to the interior of the windscreen in the cockpit. A simpler process could reduce the cost of testing.

To address this challenge, we investigate the use of a Spiral Transmission Line (STL) to detect the presence of fields leaked into a cockpit from damaged electromagnetic gaskets. The STL could be either permanently installed, or it could be temporarily placed on the windscreen during testing. To excite the field on the exterior, one could use either a second STL or a stripline. The stripline is currently used in the form of a "blanket," which is an approximate TEM transmission line.

We begin by reviewing the currently used method of testing shielding effectiveness in windows. Next, we describe various properties of STLs. We then describe two experimental configurations that use an STL to detect fields leaked into a conducting box. One uses a second STL to drive the exterior, and the other uses a stripline "blanket."

## II. Currently Used Test Method

The method currently used for testing an aperture involves driving a uniform sheet of current over the aperture, as shown in Figure 1, and as described in [1]. A resistively loaded sense wire is positioned across the aperture on the interior, and a ratio is formed between the voltage in the sense wire and the current driving the aperture.

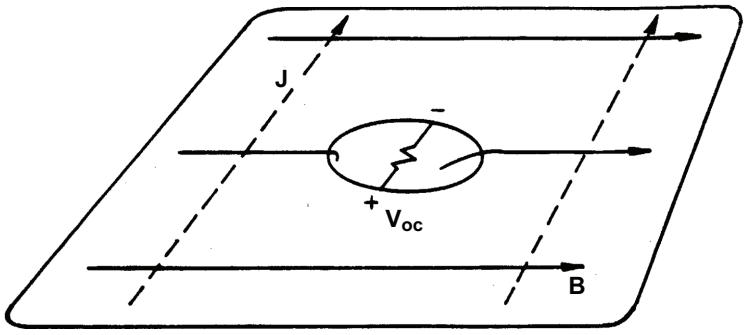


Figure 1. The currently used technique for testing apertures, from [1].

To drive the current across the aperture, one uses a stripline, as shown in Figure 2. The stripline ideally has a uniform impedance of 50 Ω, but in practice its impedance profile is nonuniform. Because this is not a uniform TEM transmission line, the excitation is not uniform with respect to frequency. Such variations can be normalized out. The stripline is mounted onto a "blanket" that is positioned over the exterior of the windscreen, and the sense wire is positioned across the interior. A current probe measures the current through the sense wire, and a network analyzer measures the transfer impedance.

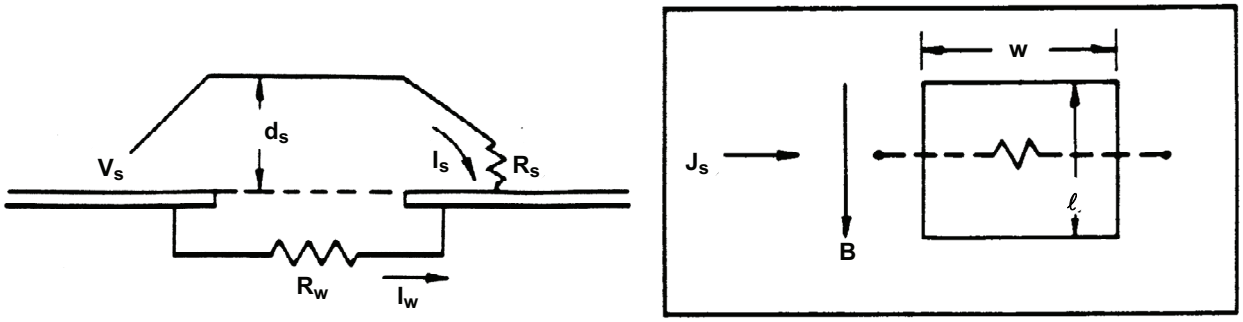


Figure 2. Currently used test fixture; side view (left) and top view (right), from [1].

## III. Properties of Spiral Transmission Lines

We consider now the properties of STLs, because they are used in our new test methods. These methods are based on the SPIRA concept described by C. E. Baum in [2]. A sketch of an STL is shown in Figure 3. They are fabricated from a coil of insulated wire, positioned very close to the ground plane, to form a slow-wave transmission line.

An STL might be used in either transmission or reception. When used in transmission, it is placed in parallel to the gasket or seam, as shown in Figure 4. A source drives the transmission line, which causes current to flow across the seam. If there are gaps in the seam, fields radiate to the other side, where they are detected. When used in reception, reciprocity applies. So fields that are leaked through the seam launch a voltage onto the STL that propagates to either end.

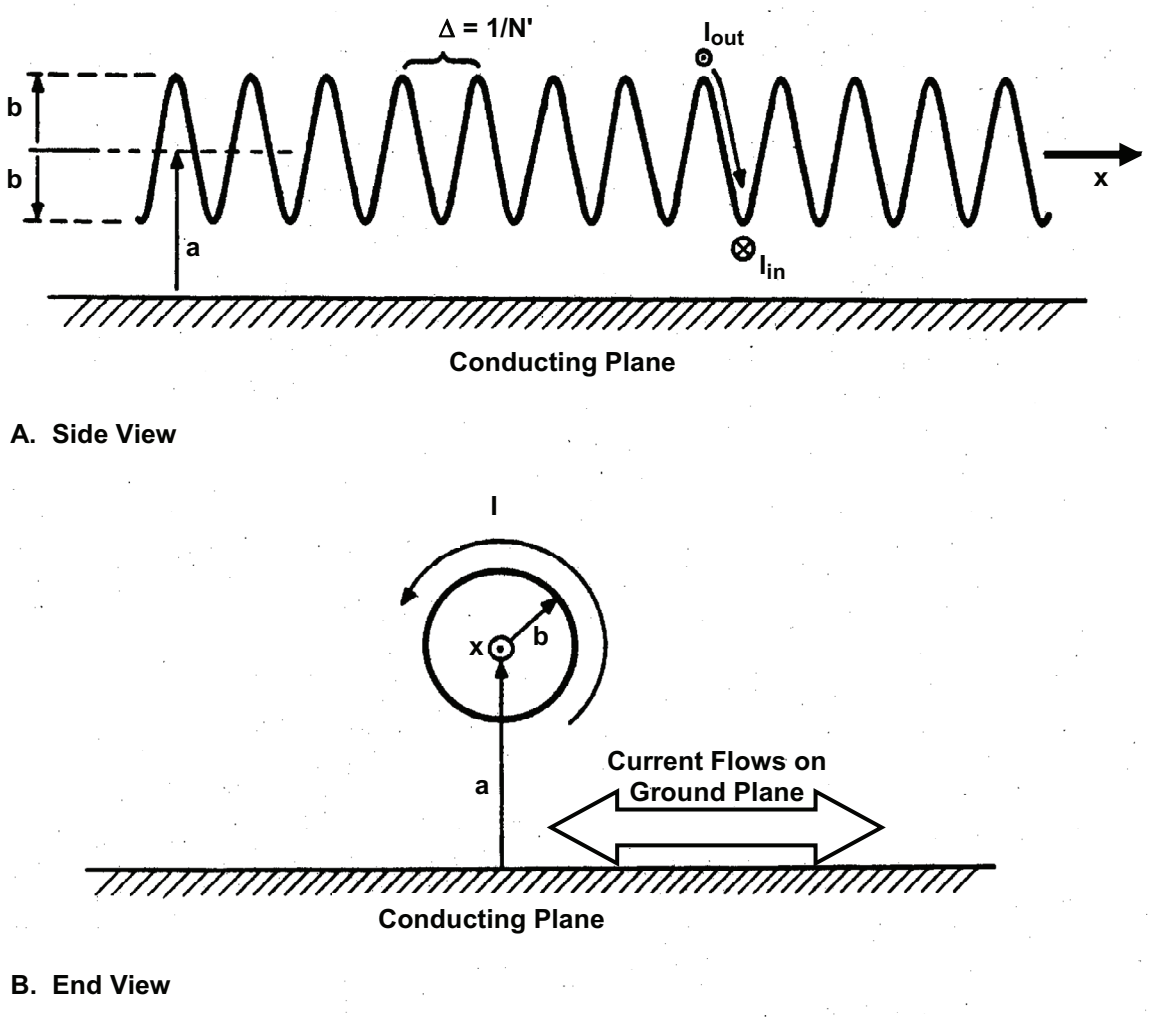


Figure 3. Spiral Transmission Line, from [2].

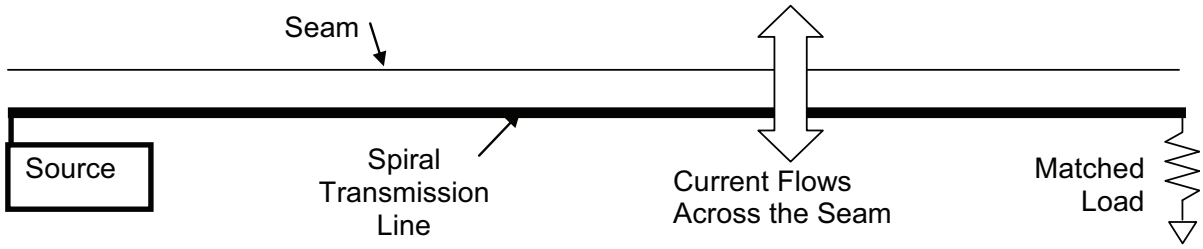


Figure 4. Interior of embedded windscreen shield monitor.

To understand why the STL causes transverse currents to flow across the seam, we consider the fields due to a solenoid. Magnetic fields run parallel to the axis on both the interior and exterior. In the presence of a ground plane, axial magnetic fields create transverse currents, described by $\vec{J} = -2\,\hat{n} \times \vec{H}$ . Thus, these transverse currents run across the seam, which causes leakage fields.

To calculate the impedance of a spiral transmission line, we start with the expressions for a cylinder above a ground plane, and we add an extra inductance due to the coil. Thus, the characteristic impedance of the line for a cylinder above ground is

$$Z_{o,cyl} = \sqrt{L_o' / C_o'} \tag{1}$$

where $L_o$' and $C_o$' are the inductance and capacitance per unit length. These are calculated as

$$L_o' = \mu_o f_g, \qquad C_o' = \frac{\varepsilon_o}{f_g}, \qquad f_g = \frac{1}{2\pi} \operatorname{arccosh}(a/b) \tag{2}$$

where $a$ is the distance from the center of the helix to the ground plane, and $b$ is the radius of the helix. Furthermore, $\varepsilon_o$ and $\mu_o$ are the permittivity and permeability of free space.

To find the impedance of the spiral transmission line, we add the inductance per unit length of the solenoid to our previous expression, leading to

$$Z_{o,spiral} = \sqrt{\frac{L_o' + L_s'}{C_o'}}, \quad L_s' = \mu_o N'^2 A \tag{3}$$

where $L_s$' is the inductance per unit length of the spiral, $N'$ is the number of turns per unit length in the spiral, and $A$ is the cross-sectional area of the spiral. Similarly, we obtain the velocity of propagation of the wave along the transmission line as

$$v_{p,spiral} = \sqrt{\frac{1}{\left(L_o' + L_s'\right)C_o'}} \tag{4}$$

Note that the above expressions are valid only when the risetime and/or wavelength of the driving function are large compared to the diameter of the spiral. In an experiment, it is simple to check the impedance and phase velocity with a Time Domain Reflectometer.

## IV. Dual STL Measurements

We tested two configurations that used an STL on the interior to detect slot leakage. One used dual STLs – one each on the interior and exterior of a metal box. The other used a stripline "blanket" on the exterior.

We describe first the experiments with dual STLs. We investigated whether it was possible to detect a leak, and if so, whether we could determine its position. Sketches of this configuration are shown in Figures 5 and 6, and photos are shown in Figure 7-9.

The conducting box had two slots, whose position we determined based on the time delay of the received signal. The two slots were designated as "Near Slot" and "Far Slot," and were located close to the ports and loads, respectively. Both slots could be either open (leaky) or closed with copper tape, depending on the experiment. The top of the box acted as a ground plane for both the interior and exterior STLs.

First, we consider characteristics of the conductive box. The dimensions of the box were 42.7 x 25 x 13 cm, and all seams were sealed with copper tape to prevent leakage. Two slots were cut into the ground plane, running parallel to the STLs. Each slot was 38 mm x 1 mm in size. The center-to-center separation between the two slots was 26.15 cm.

Next, we consider details of the STLs. Each coil was 37 cm in length, and was wound 43 turns on a wood dowel 9.5 mm in diameter, resulting in one turn every 8.6 mm. The outer diameter of the spirals was 12 mm. The windings were fabricated from 18 AWG enameled magnet wire, positioned so their insulation was in firm contact with the metal ground plane. The diameter of the enameled magnet wire was 1.05 mm, including the enamel. The STLs were positioned so the projections of their axes on the ground plane were 12 mm away from the slots.

The dual STL configuration, shown in Figure 6, works as follows. Port 1 drives the exterior STL, while Port 2 detects the fields that leak into the box through the slots. Fields that leak through the Near Slot appear earlier in time than those that leak through the Far Slot. Thus, the time of arrival can be used to determine the location of the fault. Each coil is fed by a 50-Ω coaxial cable. The characteristic impedance of each STL is 180 Ω, so a matching circuit is needed to match to a 50 Ω input cable. This is implemented simply with a 68-Ω shunt resistor to ground. The far end is terminated in a 180-Ω resistor to eliminate reflections.

We attempted to use the theory of the previous section to design the STL. However, we found the characteristic impedance was highly sensitive to small changes in height above the ground plane. To achieve a uniform impedance, we secured the spiral firmly against the ground plane, and accepted the impedance we observed — 180 Ω. Thus, the clearance between the STL and the ground plane was just the thickness of the insulation.

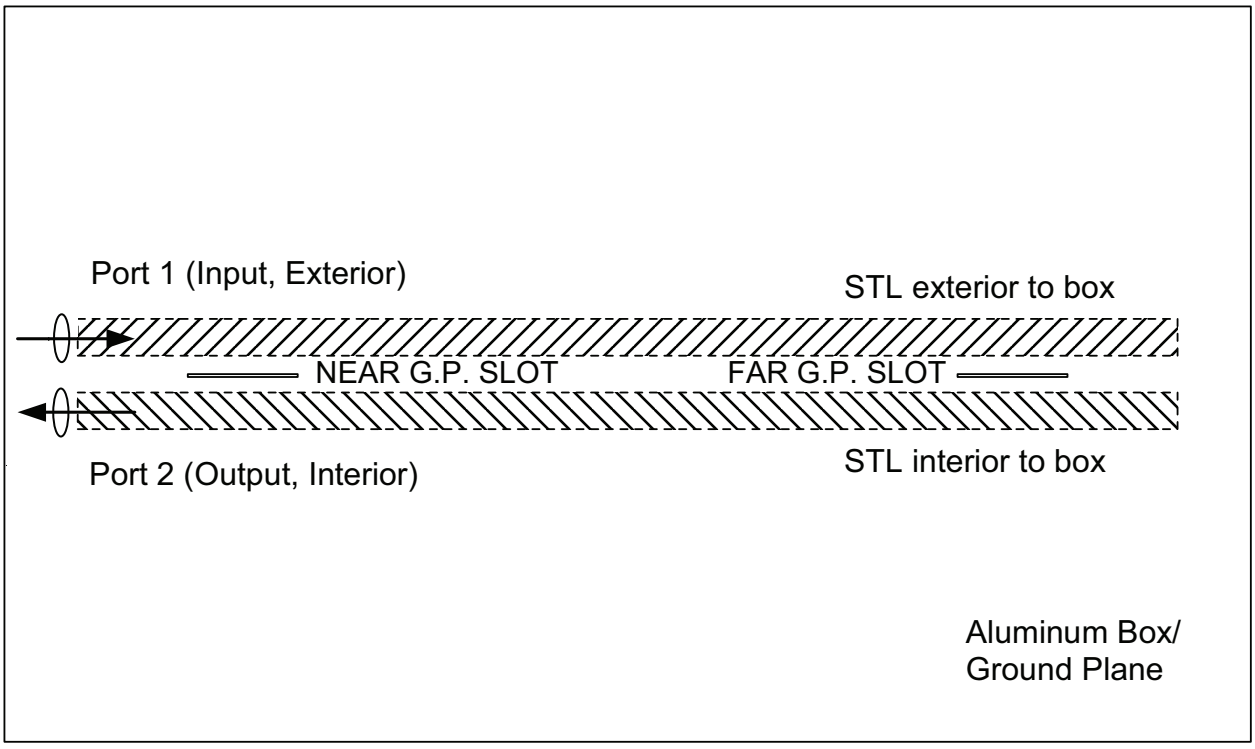


Figure 5. Layout of the dual STL measurement.

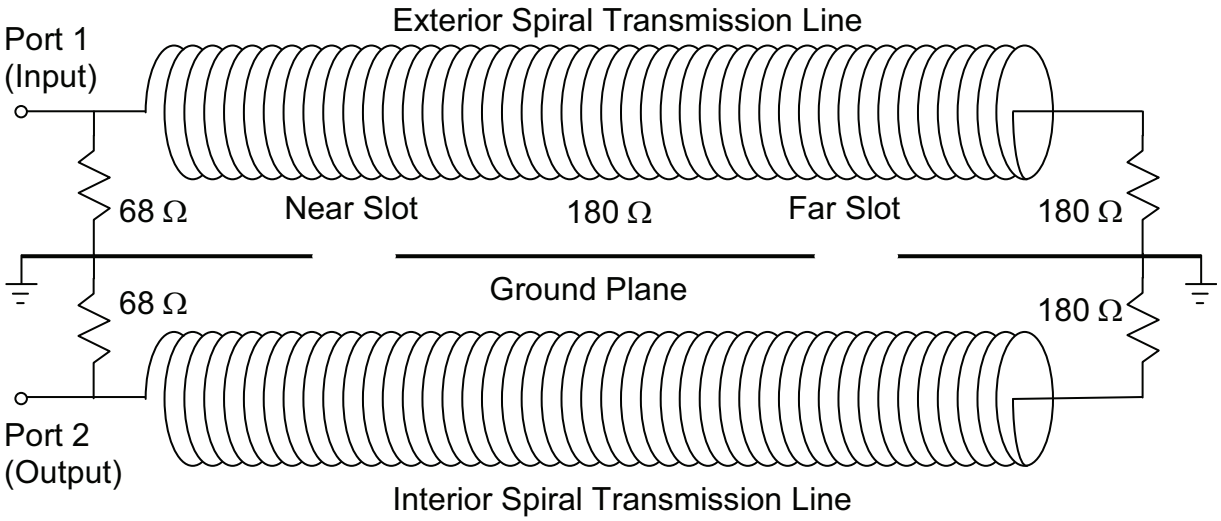


Figure 6. Circuit diagram of the Dual STL measurement. The STL forms a transmission line with a 180-Ω characteristic impedance.

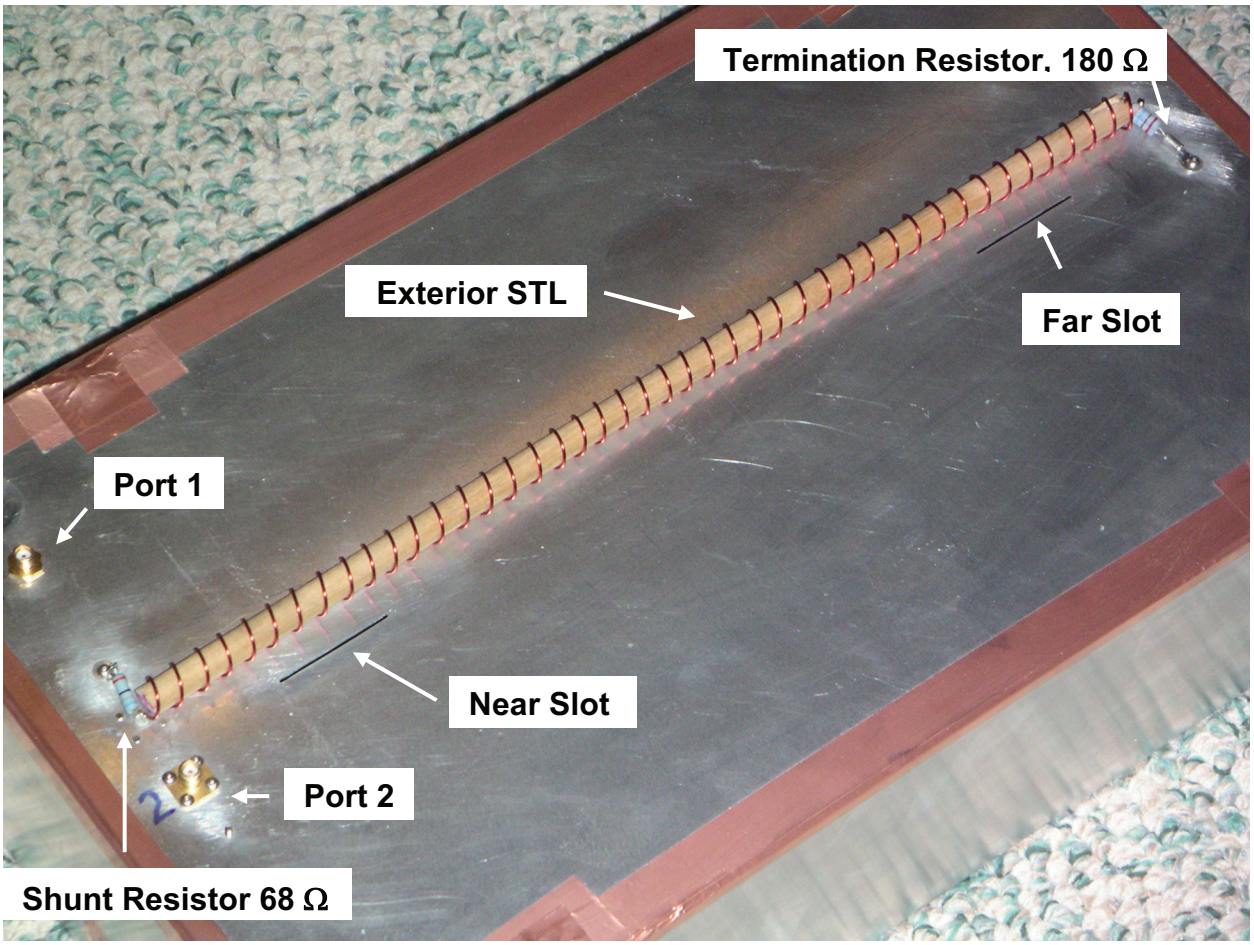


Figure 7. The exterior STL mounted onto the shielded box. The interior coil is mounted on the other side of the ground plane, parallel to the two slots, and to the right of the SMA connector labeled Port 2. Port 1 drives the upper coil through a short length of cable within the box, followed by a feed-through SMA connector on the interior.

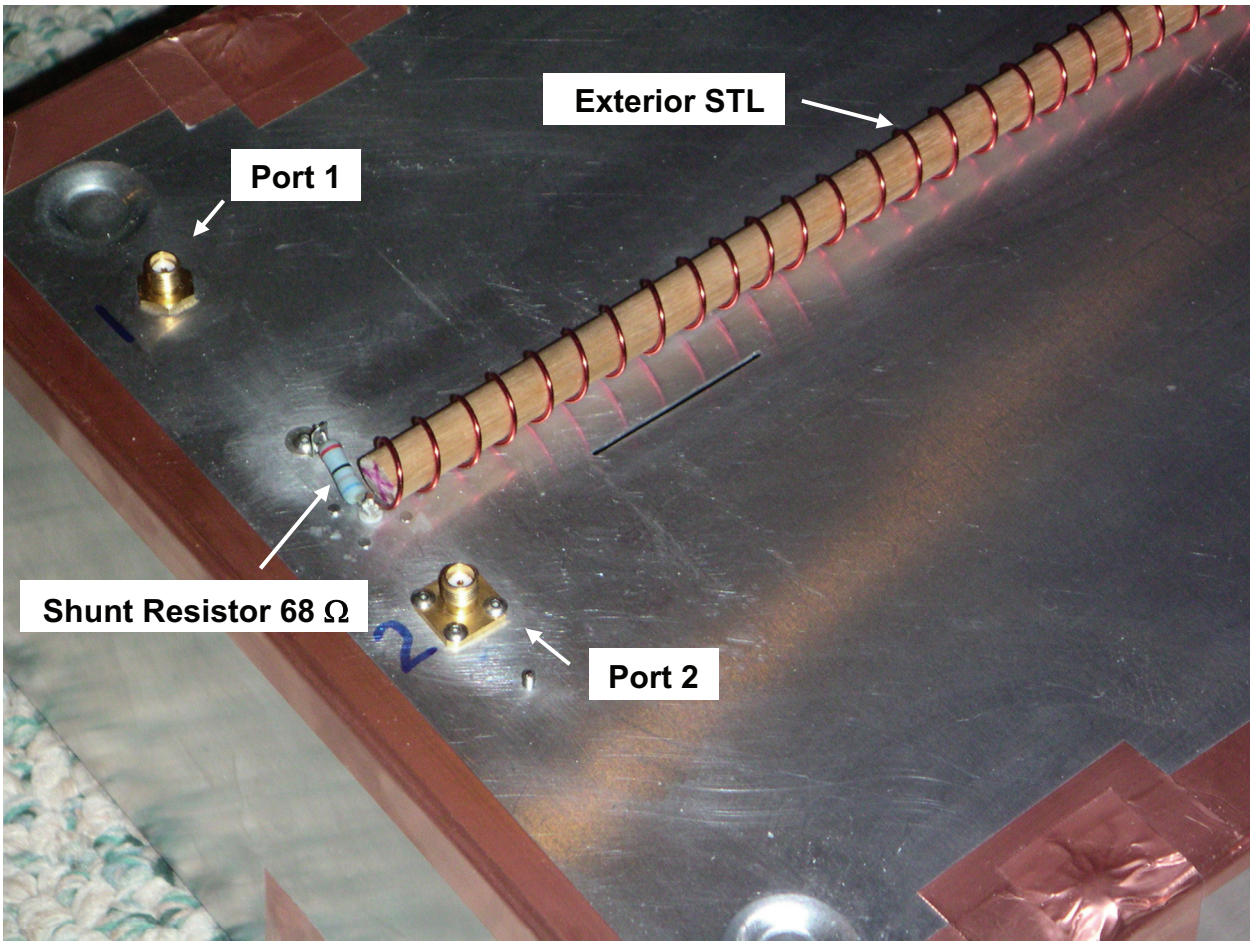


Figure 8. A close-up view of the exterior STL, showing the 68-Ω shunt resistor to ground. Note that Port 1 drives the Exterior STL through a short loop of cable within the box, followed by a feed-through SMA connector.

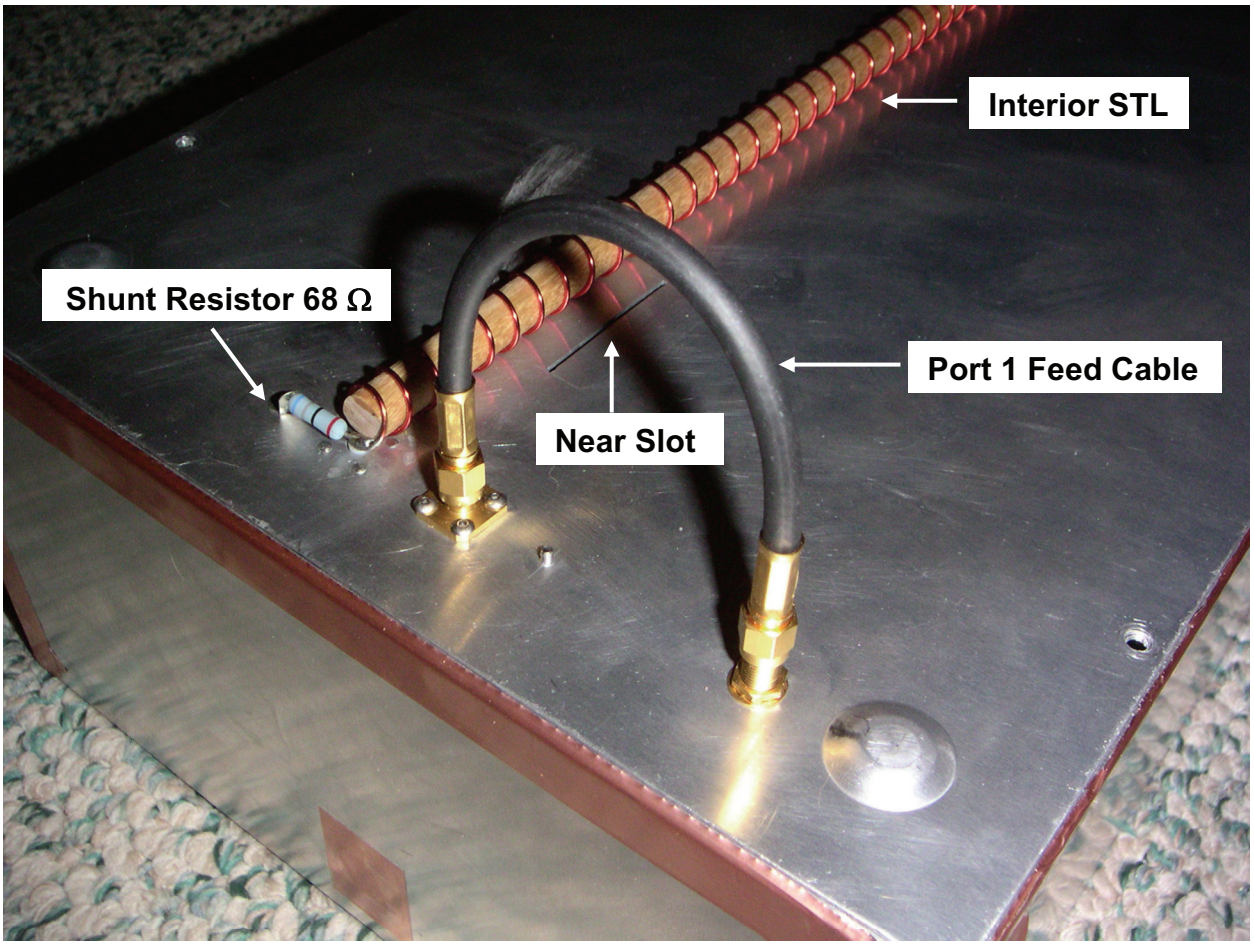


Figure 9. The shielded box with the ground plane flipped over to reveal its underside. The receiving coil is shown with its 68-Ω shunt matching resistor. The Port 1 feed cable feeds signal from Port 1 to the exterior STL, which drives the slot with a source.

We now consider the time domain results of the dual STL experiment. First, we measured the TDR of the two STLs, with both slots closed. For this, we used a Tektronix model TDS8000 sampling oscilloscope with 80E04 sampling head. After taking the data, we applied a fourth-order lowpass filter, with a 3 dB frequency of 2 GHz, and the results are shown in Figure 10. We hoped to realize a flat 50-Ω impedance profile, and that is approximately what we do see. Note that the impedance of the transmission line is actually 180 Ω, but it looks like 50 Ω because of the 68 Ω shunt resistor. Note also that there are discontinuities near both Ports 1 and 2, at the beginning of both STLs. We went through several iterations to reduce these, and this is the best we obtained.

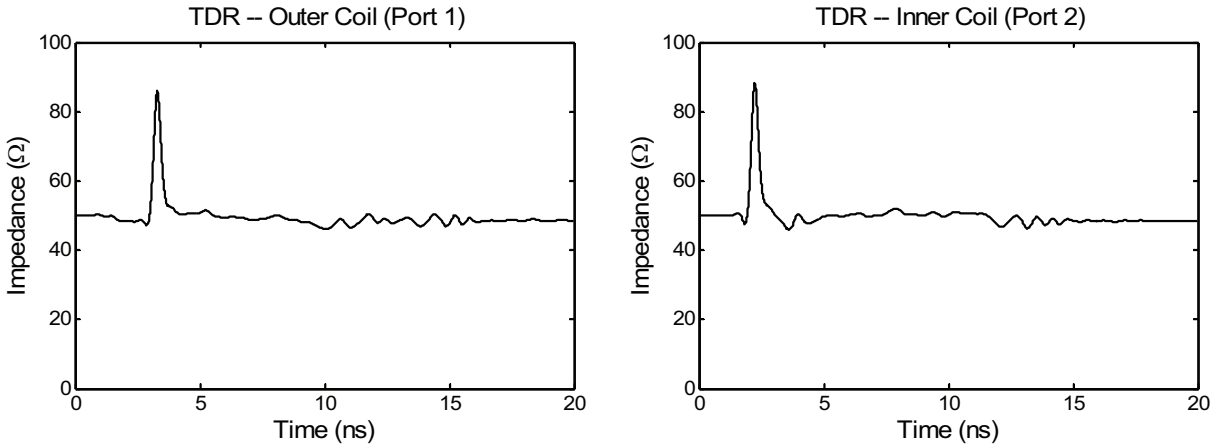


Figure 10. TDR of Port 1 (left) and Port 2 (right).

Next, we detected fields leaked through the near and far slots. We drove Port 1 with a Picosecond Pulse Labs model 2000D pulser, whose output voltage is shown in Figure 11. It has a peak voltage of 45 V, a risetime of 350 ps, and a flat top for 10 ns. We then detected the signal at Port 2 under three conditions: both slots closed, Near Slot open, and Far Slot open. The measured waveforms are shown in Figure 12.

From the data, we see that with both slots closed, there is no signal detected at Port 2. However, with either slot open, there is a clear leakage signal detected at Port 2. The peak signal occurs at different times for the two slots – 2.4 ns when the Near Slot is open, and 10.2 ns when the Far Slot is open. Thus, there is a 7.8 ns difference in time of arrival.

We can use the difference in time of arrival to find the distance between the two slots. To do so, we first measure the velocity of propagation on the STL. A perturbation placed at the far end of the line (a finger) appears on a TDR trace 11 ns after the input connector. Thus, the round-trip transit time of the STL is 11 ns. Since the physical length of the STL is 37 cm, we get the velocity of propagation as (2 x 37 cm)/11 ns = 6.7 cm/ns = 0.22 $c$, where $c$ is the speed of light in free space.

Continuing the calculation, the slots are separated by 7.8 ns round-trip on the TDR, or 3.9 ns one way. This implies that their center-to-center separation is 3.9 ns x 6.7 cm/ns = 26.1 cm. From the physical dimensions of the box, the center-to-center separation of the slots is 26.15 cm, so we are accurate to within about 0.2%.

As a result of this measurement, we see that the peak return signal can indeed be used to locate the position of a leak with high accuracy.

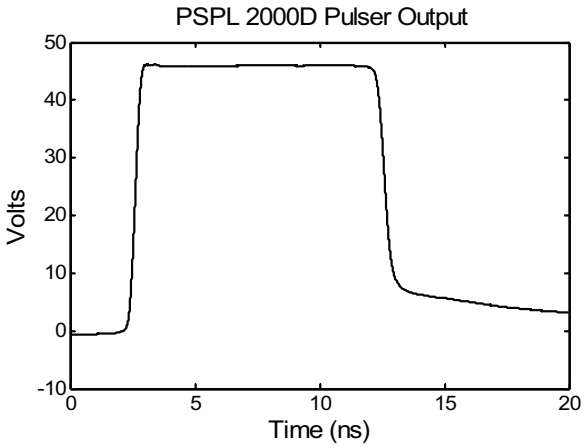


Figure 11. The output voltage of the PSPL model 2000D pulser.

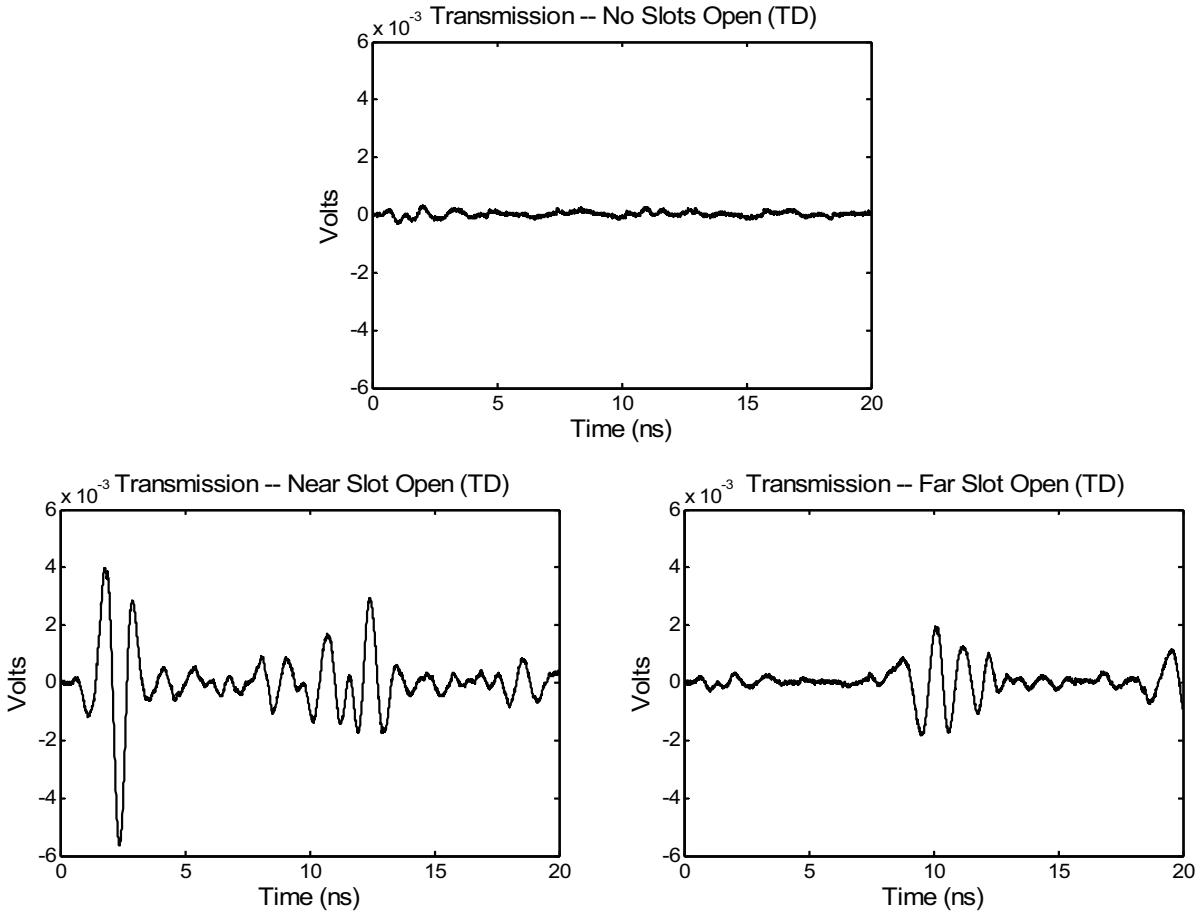


Figure 12. Leaked fields in the dual STL fixture, with both slots closed (top), Near Slot open (left), and Far Slot open (right). The peak signal occurs at 2.4 ns, with the Near Slot open, and 10.2 ns with the Far Slot open, resulting in a 7.8 ns time difference.

We next tried the same measurement in the frequency domain, using a Vector Network Analyzer (VNA) with time domain option (Agilent model 8753ES). We took data over a broad range of frequencies, and then used the internal FFT routines to convert the frequency sweeps to the time domain. The resulting time domain waveforms are shown in Figure 13, for three cases: no slots open, Near Slot open, and Far Slot open. As before, the time difference between the two signals is about 7.8 ns. Furthermore, the shape of the resulting time domain curves is very similar to those of Figure 12.

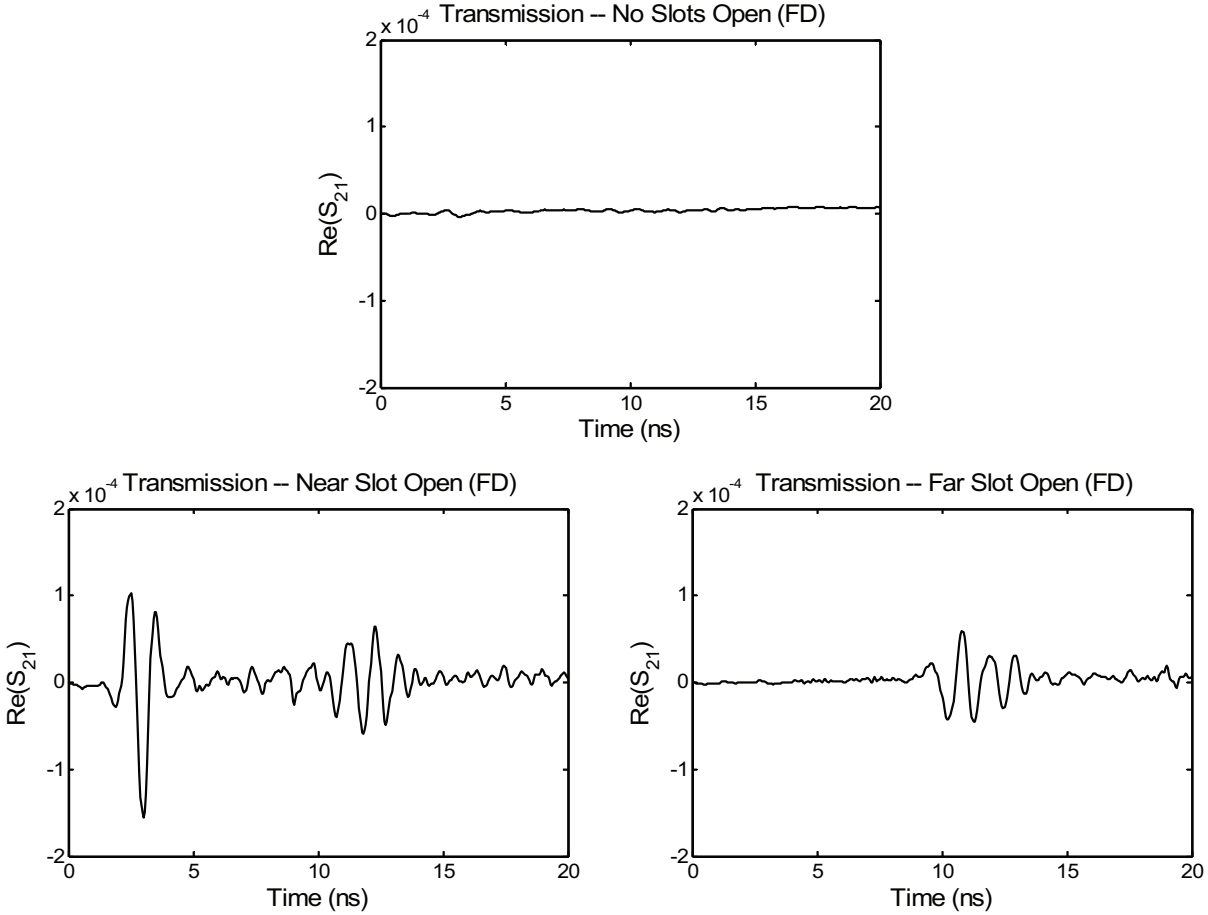


Figure 13. Leaked fields in the dual STL experiment using the time domain option on a VNA; both slots closed (top), Near Slot open (left) and Far Slot open (right). Note the similarity to the previous figure.

The above results suggest that one could use either frequency domain or time domain equipment to detect a shielding fault in a seam. We estimate that the time domain equipment would cost about half that of the frequency domain equipment. However, the frequency domain equipment might have a greater dynamic range.

We also took some conventional data with a VNA in the frequency domain. First, we measured the $S_{11}$ of Port 1 with both slots closed, as shown in Figure 14. We see that the return loss is around –6 dB or better below 450 MHz.

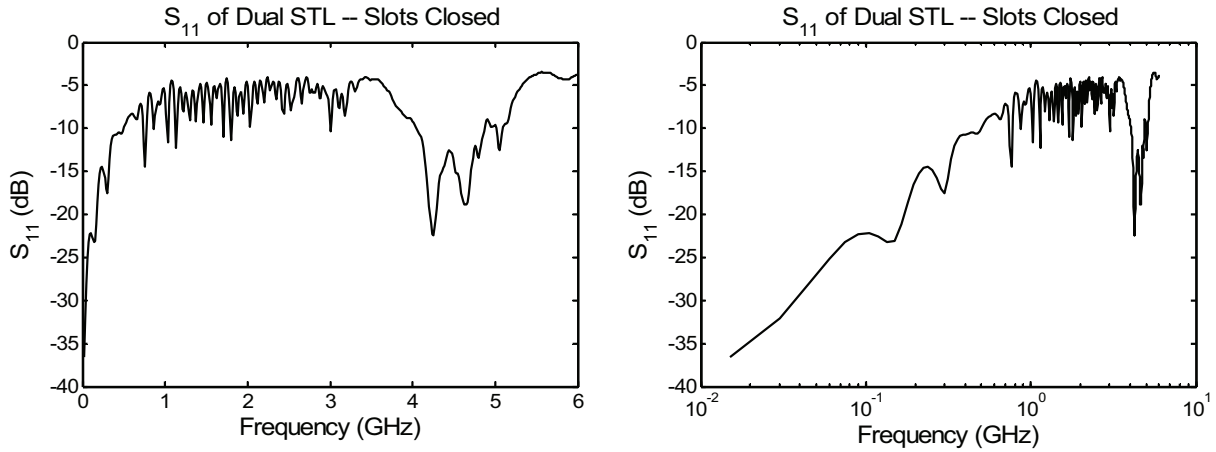


Figure 14. Return loss ($S_{11}$) of Port 1, with both slots closed.

Next, we measured the leaked fields ($S_{21}$) in the frequency domain in three configurations. These were both slots closed, Near Slot open, and Far Slot open. These results are shown in Figure 15, where we see that the two configurations with open slots have a signal that is 20 dB higher than the baseline level detected with both slots closed. So conventional VNA measurements can also be used with dual STLs to identify a shielding fault in a seam, but cannot provide location information.

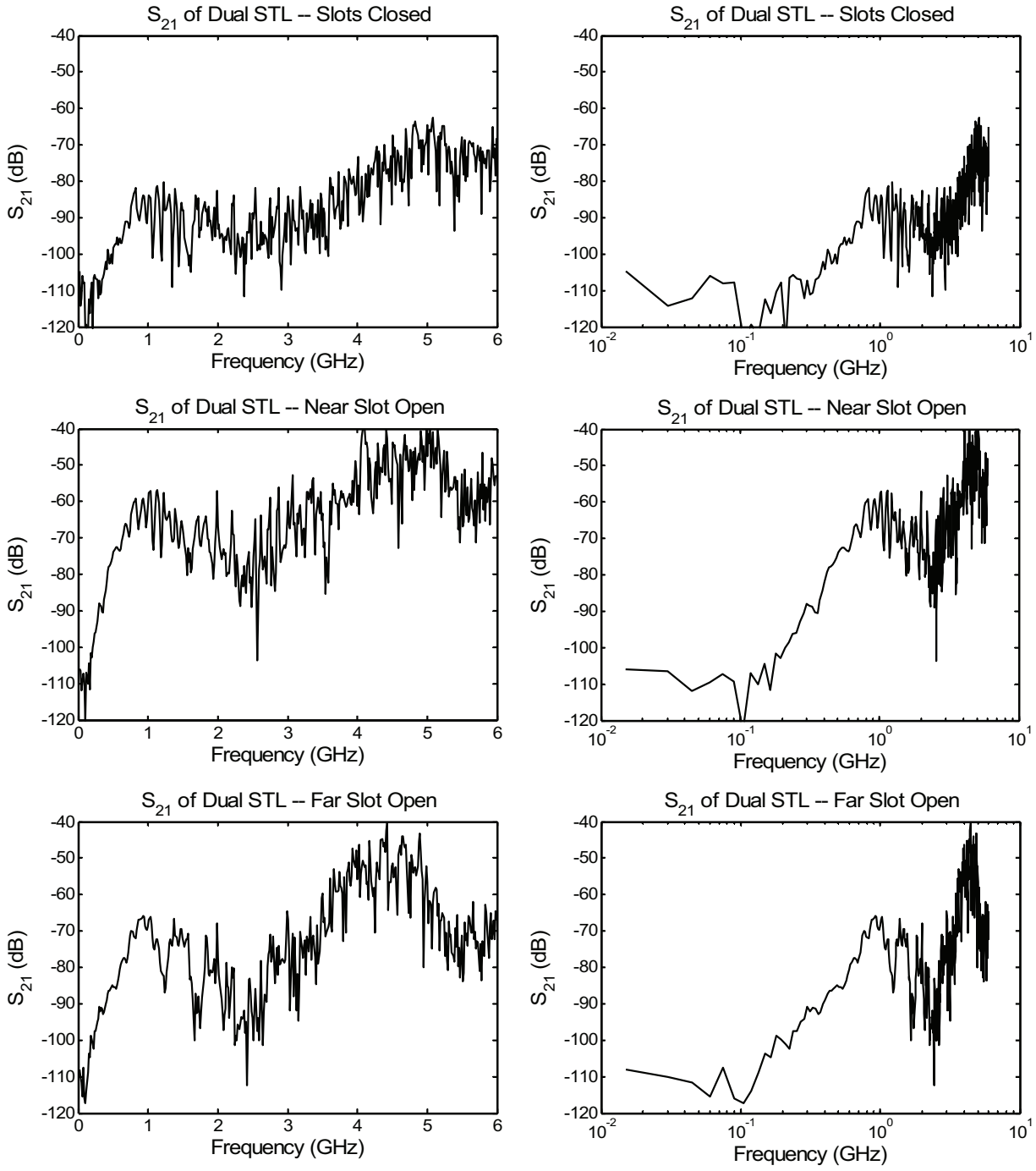


Figure 15. Leaked field ($S_{21}$) of the dual-STL experiment as measured in the frequency domain; with both slots closed (top), near slot open (middle), and far slot open (bottom).

## V. Alternative Exterior Antennas

As a variation on the dual STL configuration, we replaced the exterior STL with a variety of alternative antennas. These included a 9-in diameter half Impulse Radiating Antenna, a Farr Research model TEM-1-50 sensor [3], and an Impulse Slot Antenna [4]; all of which are shown in Figure 16. Each of these antennas was used in receive mode, while the interior STL transmitted. These tests where carried out in the time domain, using the PSPL model 2000D pulser and the Tektronix model TDS8000 digital sampling oscilloscope. All three antennas were successful in detecting leaks.

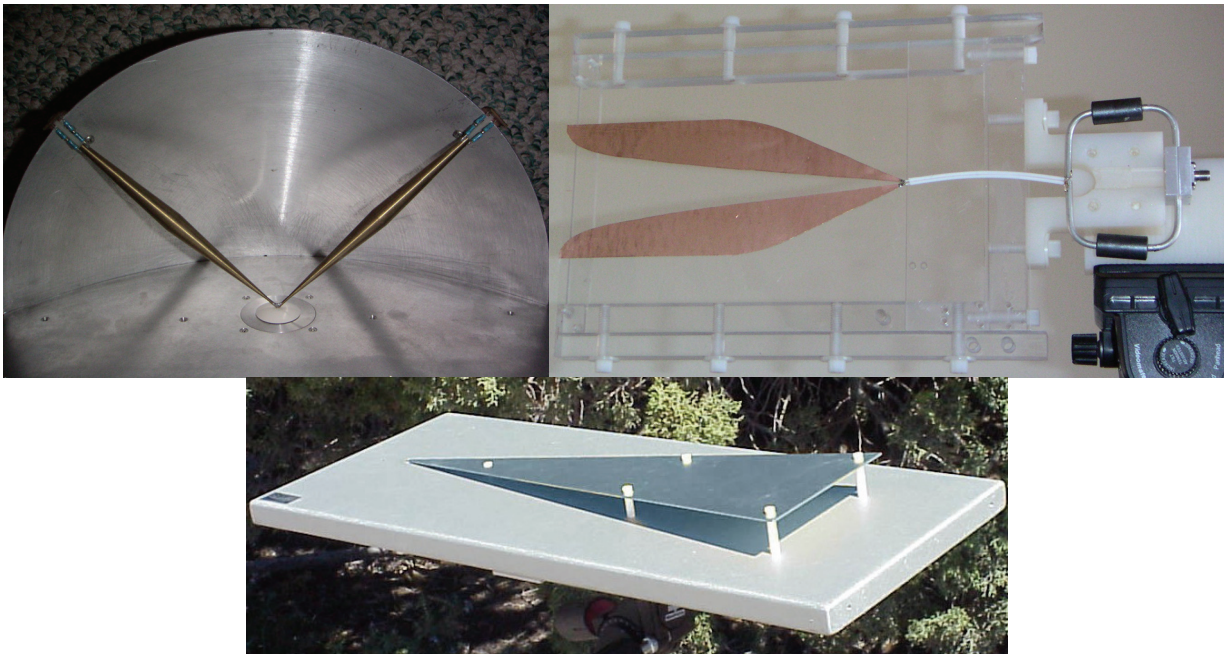

Figure 16. A collection of alternative exterior antennas used with an interior STL to detect a shielding fault: 9-inch diameter half IRA (left), Impulse Slot Antenna (right), and Farr Research model TEM-1-50 (bottom).

We conclude that a variety of exterior antennas may be used with an interior STL to detect shielding faults.

## VI. Measurements with Stripline and STL

Next, we tested for leakage with a 50-Ω stripline on the exterior, and an STL on the interior. The stripline is similar to the "blanket" that is currently used, and it excites the exterior of the aircraft, or in this case, a steel box. The STL detects the fields leaked into the box.

### A. Configuration

The steel box was a 2-foot cube, covered by an aluminum sheet with a 22.9 x 27.9 cm (9" x 11") window that was either leaky or sealed (open or closed). We drove the exterior of box with a stripline terminated in 50 Ω, as shown in Figure 17. We detected fields on the interior with an STL operating in differential mode with a balun (Prodyn model BIB-100F, 200 kHz–3.5 GHz), as shown in Figures 18 and 19. Our VNA measured the leakage signal ($S_{21}$), where Port 1 drove the stripline, while Port 2 detected the signal leaked to the interior. We compared the leakage signal for open and closed seams over 0.2–200 MHz.

In the closed configuration, all four sides of the window panel were bolted to the aluminum ground plane with nylon bolts. The bolt heads and seams were sealed with copper tape. In the leaky configuration, one short side of the panel (perpendicular to the propagation direction) was kept open with several nylon washers of thickness 0.83 mm. The copper tape was removed from that side.

Figure 17. Exterior of the box, showing the stripline (or "blanket"), terminated in 50 Ω.

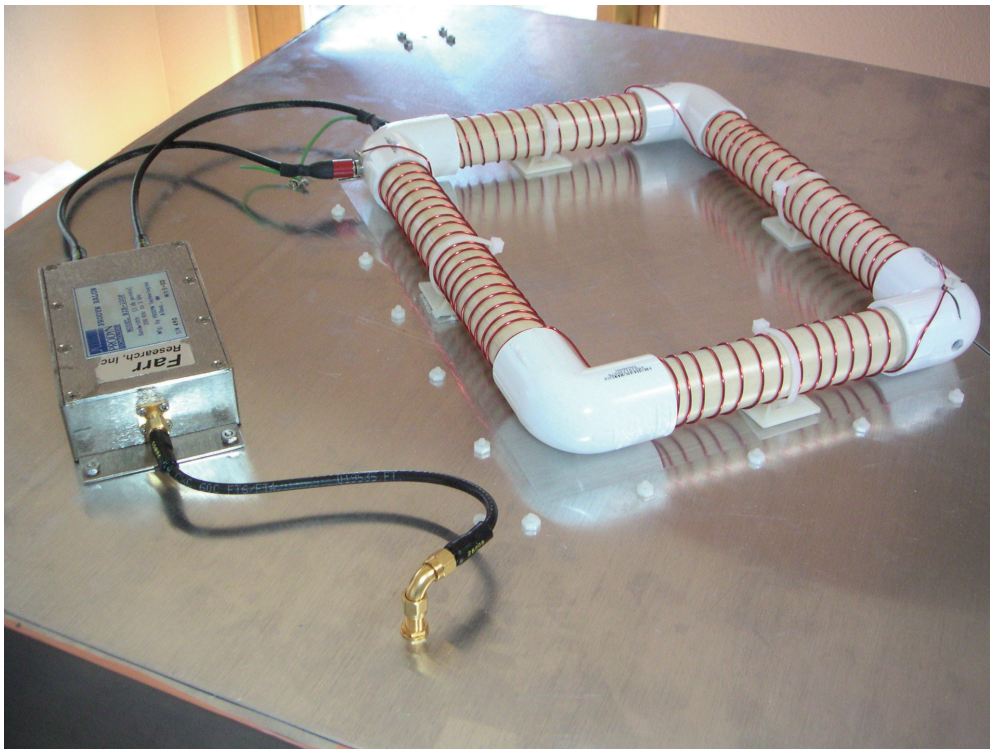


Figure 18. Interior of the box. The aluminum top panel of the box has been flipped over to show the interior. The differential signal from the STL is fed into a balun, which sums the two inputs. A cable carries the signal to the exterior through a panel-mount SMA connector.

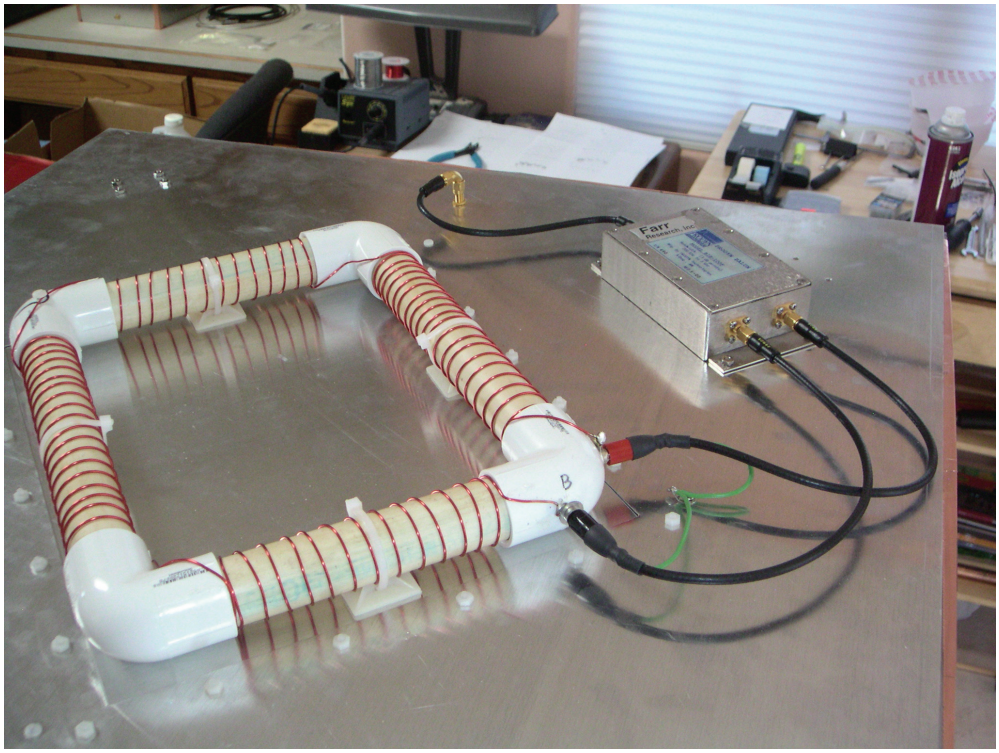


Figure 19. A second view of the interior of the box, with top panel flipped over.

The steel shield box had dimensions of 61 cm cubed (2 ft cubed). The aluminum top side of the box was the ground plane, with thickness 0.063 cm (0.025"). There was a rectangular hole in the ground plane with dimensions 27.9 x 22.9 cm (11" x 9"). This hole was covered by an aluminum window panel with dimensions 30.5 x 25.5 cm (12" x 10") and with a thickness of 0.063 cm (0.025").

On the exterior of the box was a stripline with dimensions 30 x 30 cm, positioned 6 cm above the ground plane. This was supported on four nylon posts located near the corners of the window opening. Triangular sections provided smooth tapers to points on the ground plane located 65 cm apart, where SMA connectors were mounted. Thus, along with the ground plane, the stripline formed an approximate 50-Ω transmission line.

The stripline can only test for leaks in seams that run perpendicular to the direction of propagation. Therefore, one must be able to rotate the stripline by 90°, so it can test both horizontal and vertical seams. Our stripline had this capability, but it was not used, because we only tested a single leaky seam.

On the interior of the box, the STL was mounted onto the window panel. The coil was lacquered magnet wire, 1.05 mm in diameter, wrapped around four segments of plastic pipe, with a diameter of 26.8 mm. The axes of these four pipes formed a rectangle 19 cm x 24 cm. The lengths of the coil segments were 11.4 cm along the short dimension and 16.5 cm in the long dimension. The short segments consisted of 13 turns, while the long segments were 20 turns. The average spacing between turns was 0.85 cm, and the coil sections were 28.9 mm in diameter. When mounted on the window panel, the clearance between the coil and the panel surface was 5.78 mm.

The windings on the coil required some special features. The coil segments were connected in series, with straight sections of wire bridging the gaps between segments. The winding started and ended at one corner of the rectangle. The winding direction was reversed at the corner diagonally opposite the feed. This was done so signals from opposite sides of the window would add constructively, instead of cancelling each other out.

### B. Results

First we recorded the TDR of the stripline, as shown in Figure 20. This was filtered with a fourth-order lowpass filter with a cutoff frequency of 1 GHz. We hoped to see a flat 50 Ω, and that is approximately what we observe. However, there was some deviation at the SMA connectors. We estimate that this had little effect on the experiment.

Next, we tested for leakage with the seam opened (leaky) and closed, and our results are shown in Figure 21. We observed a 30-40 dB difference in signal between the open and closed configurations over 50-200 MHz. These data demonstrate the effectiveness of the proposed method.

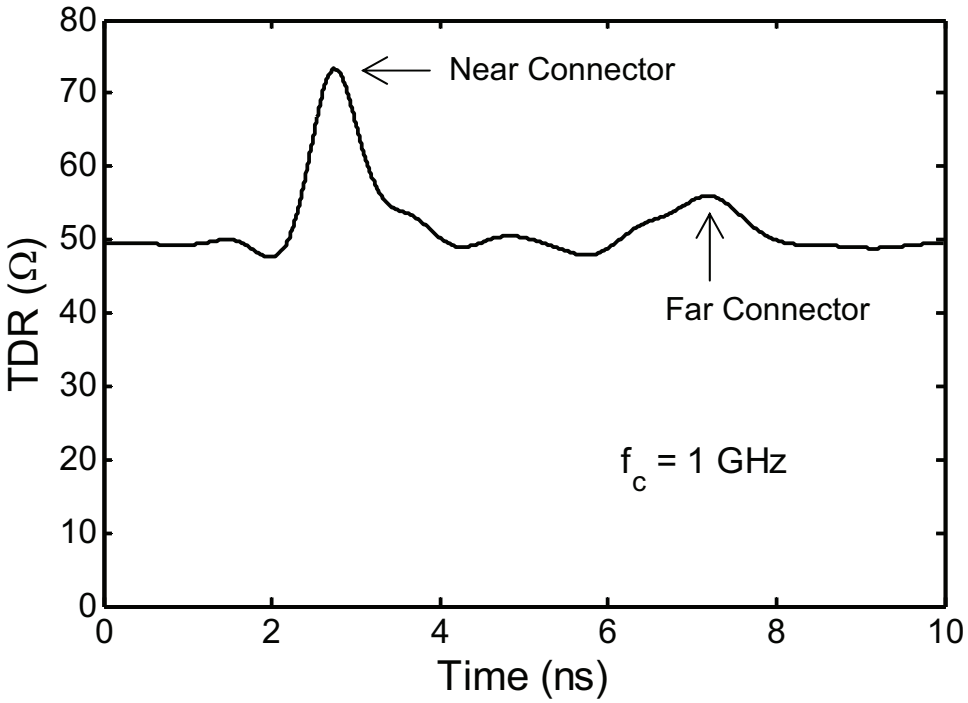


Figure 20. TDR of the stripline.

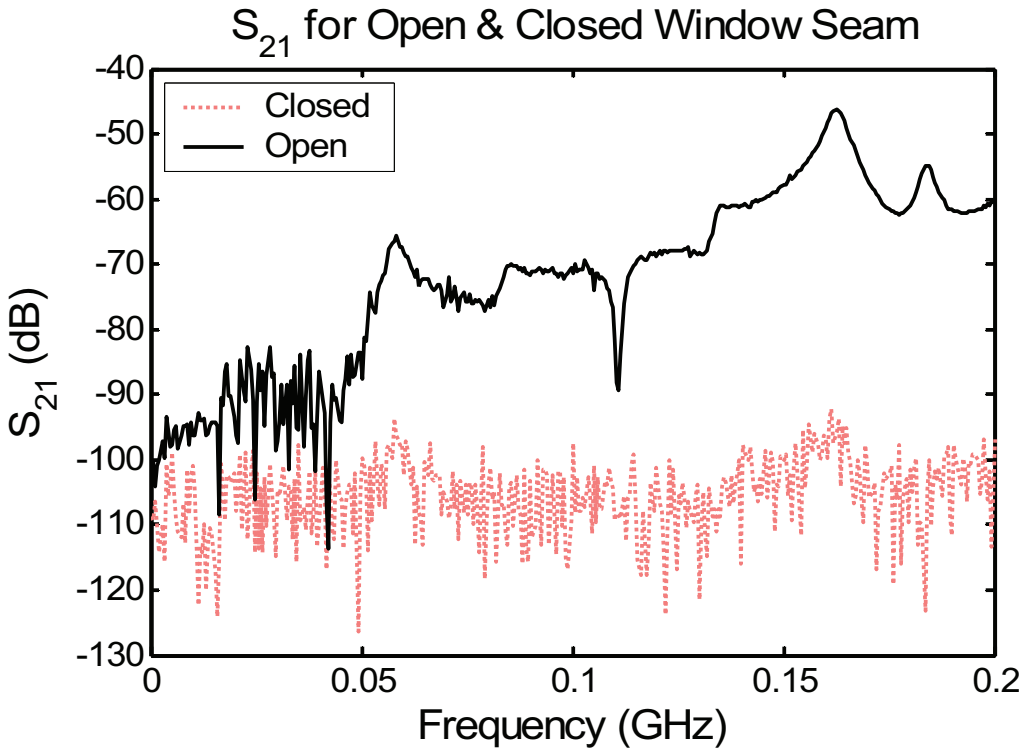


Figure 21. Comparison of leakage signals for open and closed window seams.

Finally, we recorded all four S-parameters, as shown in Figure 22. We observe that resonances in the $S_{21}$ measurement of Figure 21 also appear in the $S_{22}$ measurement of Figure 22. This indicates that the resonances in Figure 21 are coming from the STL – not the stripline. We should try to eliminate these resonances, if possible, in future experiments.

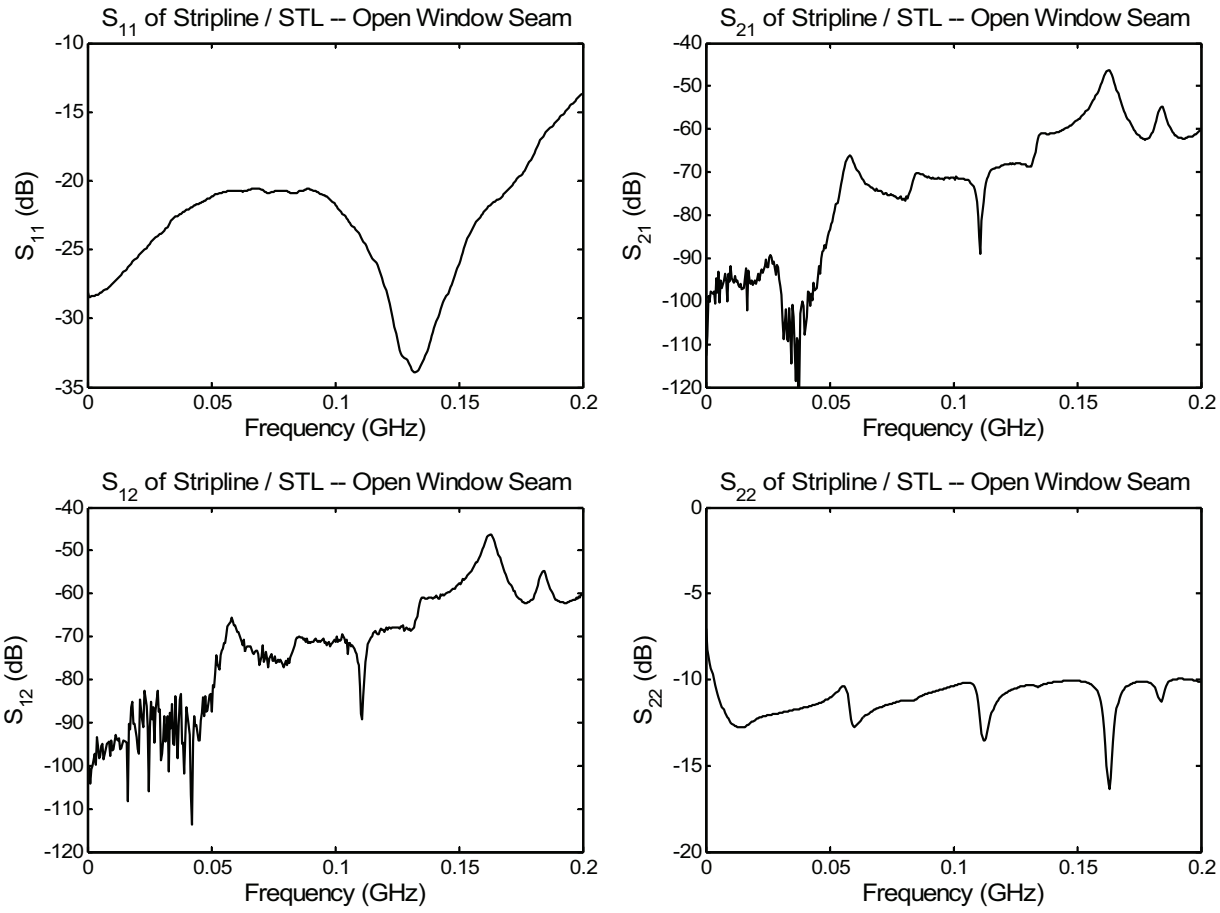


Figure 22. Plots of all four S-parameters for a leaky window. Clockwise from upper left, $S_{11}$, $S_{21}$, $S_{22}$, and $S_{12}$.

## VII. Discussion

We have successfully detected leakage through slots using an STL on the interior, and a variety of antennas on the exterior. These include a second STL, a 9-in diameter half IRA, a Farr Research model TEM-1-50 sensor, an Impulse Slot Antenna, and a stripline similar to the "blanket" that is currently used.

We have also used a variety of test methods to detect the presence of a leak. These include time domain measurements, frequency domain measurements, and frequency domain measurements converted to the time domain. Furthermore, the two time domain methods found the relative position of the leaks to an accuracy of 0.2%, when used with dual STLs.

A number of issues remain for future work. It will be of interest to test the effect of various physical parameters of the STL, including coil diameter, wire diameter, winding density, and coil height. One might also test the effect of the seam length and width. Next, one might test the effect of the feed mode of the STL – differential mode vs. single-ended mode. One might also investigate the reason for the resonances in the STL, and attempt to eliminate them as much as possible. It would also be useful to investigate the optimal frequency range over which measurements should be made.

Finally, one would want to compare our proposed method to that which is currently used. In doing so, one would want to confirm that the proposed method is simpler to implement, and that it provides similar test results. One would want to carry out this comparison on both scale models and full-size aircraft.

## VIII. Conclusions

We investigated two new methods of testing for electromagnetic leaks in windscreen gaskets using STLs on the interior. The first method, using a second STL on the exterior, offers the possibility of locating the position of a leak using time domain measurements. The second method, using a stripline on the exterior, shows a 30-40 dB leakage signal above the noise level. Much work is left to be done, as is discussed in Section VII.

## Acknowledgement

We wish to thank Jesse Sanchez of USAF, OC-ALC/LGK, Tinker AFB, for funding this work as a Phase I Small Business Innovative Research project.

## References

1. W. D. Prather and C. D. Taylor, Verification of the EMP Hardening of Aircraft Windows and Doors, Hardness Surveillance Memo 2, June, 1987.

2. C. E. Baum, A Spiral Transmission-Line Technique for Detecting Slot Apertures in Shield Enclosures, Measurement Note 37, December 1987.

3. Farr Research Inc. Catalog of UWB Antennas and HV Components, available online at www.Farr-Research.com.

4. W. S. Bigelow, *et al*, Development of the Impulse Slot Antenna (ISA) and Related Designs, Sensor and Simulation Note 505, December 2005.